



# Material properties of the Ce<sup>3+</sup>-doped garnet phosphor for a white LED application

Myoung Su Jang, Yong Ha Choi, Shulu Wu, Tae Gil Lim & Jae Soo Yoo

To cite this article: Myoung Su Jang, Yong Ha Choi, Shulu Wu, Tae Gil Lim & Jae Soo Yoo (2016) Material properties of the Ce<sup>3+</sup>-doped garnet phosphor for a white LED application, Journal of Information Display, 17:3, 117-123, DOI: [10.1080/15980316.2016.1205527](https://doi.org/10.1080/15980316.2016.1205527)

To link to this article: <https://doi.org/10.1080/15980316.2016.1205527>



© 2016 The Korean Information Display Society



Published online: 14 Jul 2016.



Submit your article to this journal [↗](#)



Article views: 1325



View related articles [↗](#)



View Crossmark data [↗](#)



Citing articles: 19 View citing articles [↗](#)

# Material properties of the $\text{Ce}^{3+}$ -doped garnet phosphor for a white LED application

Myoung Su Jang, Yong Ha Choi, Shulu Wu, Tae Gil Lim and Jae Soo Yoo

Graduate School of Chemical Engineering and Materials Science, Chung-Ang University, Seoul, Republic of Korea

## ABSTRACT

The luminous flux of the phosphor-converted white-light-emitting diode (WLED) is correlated to the optical properties of a phosphor, such as the excitation band, emission spectrum, and decay time. Also, the crystallinity, particle size, and morphology may influence the device performance, such as the luminous flux, as well as the device longevity and efficiency. The device application of the  $\text{Ce}^{3+}$ -activated  $\text{Y}_3\text{Al}_5\text{O}_{12}$  garnet phosphor was limited because of its strong patent. Its patent is set to expire in the year 2017, and the high-power operation of the WLED is becoming important. To obtain insights regarding its usability,  $\text{Y}_3\text{Al}_5\text{O}_{12}:\text{Ce}^{3+}$  phosphor was synthesized through flux-assisted solid-state reaction. It was found that this garnet phosphor has a very stable crystal structure and is inert in the processing environment. Its quantum yield reached 95%, and no photosaturation was shown within the measurement limit. It was also found that the synthetic procedures are very straightforward and that the particle size may be easily controlled. The luminous flux of the WLED was maximum when  $17.7\ \mu\text{m}\ \text{D}_{50}$  was used.

## ARTICLE HISTORY

Received 28 March 2016  
Accepted 16 May 2016

## KEYWORDS



LED; yttrium aluminum garnet; photosaturation; flux; phosphor

## 1. Introduction

The white-light-emitting diode (WLED) has been widely used as a solid-state lighting source in various application fields. Compared to the traditional lighting, WLED has well-defined advantages, such as high efficiency, long lifetime (over 100,000 h), energy savings, and easy light quality control. Above all, its environmental-protection support and design flexibility have been the main driving forces for the growth of its market share [1–3]. After its successful application to the LCD backlight, streetlights, indoor illumination, and car lights have become important application sectors for this high-end LED product, which may be due to its easy light quality control and design flexibility.

After Nichia Corporation, which was once a small chemical company, announced its pioneering work on the blue-light-emitting diode, a group of engineers in the same company developed a WLED by coating a blue diode chip with yellow-light-emitting phosphor ( $\text{Y}_3\text{Al}_5\text{O}_{12}:\text{Ce}^{3+}/\text{YAG}:\text{Ce}$ ). As is well known, a series of works has led to a powerful rights and even to 2014 Nobel laureates in physics. Also, this technology breakthrough made Nichia Corporation one of the most influential

companies protected by patents in the world. Yttrium aluminum garnet ( $\text{Y}_3\text{Al}_5\text{O}_{12}$ ) is a synthetic crystalline of the garnet group. The luminescence properties of cerium-doped yttrium aluminum garnet (YAG:Ce) was first reported in the 1960s, and it was used as a phosphor in cathode ray tubes for radar application because of its fast decay time [4]. YAG:Ce phosphor is very stable due to its crystal structure and because its synthetic route is very straightforward. Also, it is quite excellent for blue-chip excitation, with its high photoluminescence quantum yield.  $\text{Ce}^{3+}$ -doped YAG exhibits yellow-light emission from the characteristic 5d and 4f energy levels. The energy levels of the  $5d^1$  excited states and the emission photon energy of  $\text{Ce}^{3+}$  ion strongly depend on the host crystals via the crystal-field-induced energy level splitting of the  $5d^1$  orbital. Combined with a blue InGaN LED, Ce-doped YAG has been successfully used in WLED [3]. The first WLED device that was reported by Nichia Corporation was composed of the chip that emits blue light and phosphors excited by blue light to emit yellow light. The human eyes sense the addition of blue and yellow light as white light. As the WLED device was once characterized by high luminous intensity, the

**CONTACT** Jae Soo Yoo  [jsyoo@cau.ac.kr](mailto:jsyoo@cau.ac.kr)  Graduate School of Chemical Engineering and Materials Science, Chung-Ang University, 84 Heukseok-Ro, Dongjak-Gu, Seoul, Republic of Korea

ISSN (print): 1598-0316; ISSN (online): 2158-1606

quality of the phosphors played a vital role in the performance of the WLED device. To make things worse, the use of  $\text{Ce}^{3+}$ -doped YAG phosphor has been limited by a patent issue. The yellow-light-emitting alternative phosphors are the silicate-based phosphor [5,6],  $\text{Ce}^{3+}$ -doped  $\text{Tb}_3\text{Al}_5\text{O}_{12}$  phosphor, and oxynitride [7,8]. The optical properties of  $\text{Ce}^{3+}$ -doped YAG phosphor, however, are superior to those of any other material. In any case, the quality of the light from the WLED has dramatically improved through the selection of various proper phosphors [9].

The typical phosphor is the other garnet,  $\text{Lu}_3\text{Al}_5\text{O}_{12}:\text{Ce}^{3+}$  phosphor, which has a broad spectrum of green to orange light, and has very good stability. With these garnet phosphors, the proper performance of the WLED was limited particularly in terms of the color rendering index and color gamut. These drawbacks have been overcome by adding suitable phosphors to packaged LEDs depending on the application sector (i.e. general lighting and lighting source for the liquid crystal display). Such phosphors are green-light-emitting  $\beta$ - $\text{SiAlON}:\text{Eu}^{2+}$  ( $\text{Si}_{6-z}\text{Al}_z\text{O}_z\text{N}_{8-z}$ , where  $z$  represents the number of Al-O pairs substituting for the Si-N pairs) [10] and red-light-emitting  $\text{CaAlSiN}_3:\text{Eu}^{2+}$  [11] and  $\text{K}_2\text{SiF}_6:\text{Mn}^{4+}$  [12].

Fortunately, the WLEDs have not reached their full potential in terms of functionalities and performance. They are widely used as a light source of the LCD backlight as well as the general lighting at department stores, public office buildings, and even the art exhibition rooms at museums. In these existing application fields, new application fields such as horticulture, biological-driven lighting, lighting in combination with daylight systems, or projection systems for illumination are increasingly being explored [13]. In these applications, very stable garnet phosphors are again drawing much attention. Besides, it is known that the patent filed by Nichia Corporation will expire in 2017, and these excellent materials are available to any user and for any application.

In this study, the optical properties of WLED were re-examined in terms of applicability, and the synthetic procedures were investigated for performance enhancement [13–15].

## 2. Experiment

The  $\text{Ce}^{3+}$ -activated phosphor  $\text{Y}_3\text{Al}_5\text{O}_{12}:\text{Ce}^{3+}$  was synthesized with solid-state reactions. Good-performance  $\text{Y}_3\text{Al}_5\text{O}_{12}:\text{Ce}^{3+}$  can be obtained through the process of high-temperature synthesizing and ball grinding. In this study, much attention was given to the flux materials for promoting complete reactions. The raw materials  $\text{Y}_2\text{O}_3$  (Qiandong, 99.999%),  $\text{Al}_2\text{O}_3$  (Alfa Aesar, 99.99%),

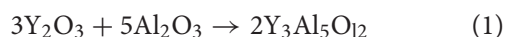
$\text{CeO}_2$  (Qiandong, 99.9%), and selected flux materials were mixed by stoichiometric proportion and were ball-milled in an isopropyl alcohol medium. After the mixing, the paste was dried in a  $100^\circ\text{C}$  oven to evaporate the medium. This pre-treated mixture was transferred to a loosely sealed alumina crucible, and then to the reactor. The rate of temperature increase in the reactor was  $3^\circ\text{C}/\text{min}$ . The prepared sample was fired at  $1500^\circ\text{C}$  for 5 h. The product was thoroughly ground and was then cleaned with 20% nitric acid for 40 min to remove the remaining reactant residues and flux materials. After the removal of the nitric acid, the product was dried at  $100^\circ\text{C}$ . The synthesized phosphors were characterized through powder X-ray diffraction (XRD; Bruker, New D8-Advance-AXS, 40 kV and 40 mA) using Cu-K $\alpha$  radiation. The room-temperature photoluminescence emission (PL) and excitation (PLE) spectra were recorded using a photomultiplier tube and a Xenon lamp (PSI, South Korea). The microstructure characteristics of the phosphors were imaged using a field emission scanning electron microscope (FE-SEM) (Thermoscientific, USA). Also, a measurement system was set for investigating the behavior of photosaturation at a high current injection in the LED packaging process. High-extraction silicon (DOW CORNING, OE6631) was used for LED packaging. The silicon resin was mixed with the synthesized  $\text{Y}_3\text{Al}_5\text{O}_{12}:\text{Ce}^{3+}$  phosphor at various ratios. Then the composite was used to coat the LED chip. The pressure and the duration time of the output were controlled with a dispenser (MUSASI Co.). During the process, the air bubble in the epoxy composite was removed using a defoamer from MUSASI Co. Finally, the packaged LED was cured at  $150^\circ\text{C}$ , and the silicon resin with phosphor was hardened. The luminous flux (lm), CRI, NTSC, and CIE of the packaged LED were measured using an integrating sphere (PSI, South Korea).

## 3. Results and discussion

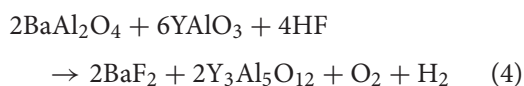
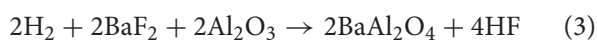
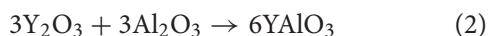
The phosphor must have a pure crystal phase with high crystallinity and few surface defects. Furthermore, the powder morphology and the distribution of the phosphor powder size are considered for device application. In general, the spherical shape is preferred for preventing scattering loss in epoxy resin. Also, the non-aggregation of the phosphor particles can increase the brightness of the packaged LED compared to the irregular-shaped particles. The particle size and distribution are directly related to the light extraction and angular color uniformity. For the ceramic phosphor plates, submicron YAG phosphors are known to be the preferred starting material. All these are dependent, however, on the synthetic route.

Generally, there are several methods of synthesizing YAG crystals. Macro-scale YAG single crystals have already been successfully grown using the slow-cooling method. This single-crystal growth technique, however, is unsuitable for phosphor powder production. Wet chemical preparations such as the hydrothermal, sol-gel, and co-precipitation methods and emulsion synthesis are mainly used to synthesize the phosphor particles. Nanoparticles are poorly crystallized and have huge specific surface areas, which result in low luminescent intensity and severe agglomeration even after calcination. Ball-shaped particles can be obtained through the spray pyrolysis method. Despite this, the emission intensity is not good enough, and the synthesis process is too complex. High-temperature solid-state reaction is the most common method of synthesizing YAG particles, even though some of the samples prepared through this method are not satisfactory. Considering its simplicity and ease of industrialization production, however, the procedure of solid-state reaction is worth refining to obtain YAG phosphor particles with a qualified morphology. In this method, particle size and shape control is the key problem for investigations.

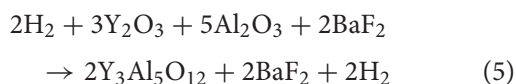
In this study, a high-temperature solid-state reaction with a proper flux was employed to prepare YAG:Ce phosphors. It is known that the mechanism of  $Y_3Al_5O_{12}$ : $Ce^{3+}$  synthesis is as follows:



When  $BaF_2$  is used as a flux, the mechanism and the effect of  $SrF_2$  can be summarized as follows:



Reorganizing the above formulae,



The mole ratios among  $Y_2O_3$ ,  $Al_2O_3$ , and  $BaF_2$  were set to be 3:5:2, but among the optimum mole ratios for the maximum luminous intensity, the best mole ratios were experimentally determined. For instance, the maximum intensity was obtained when  $BaF_2$  was 25 mol%. Based on this mechanism, it is worth noting that the crucible for the raw materials is kept in the proper environment: a loosely sealed crucible that functions to prevent the  $F_2$  gas from escaping. This sealing process is an important variable. A non-sealed crucible was experimented on to

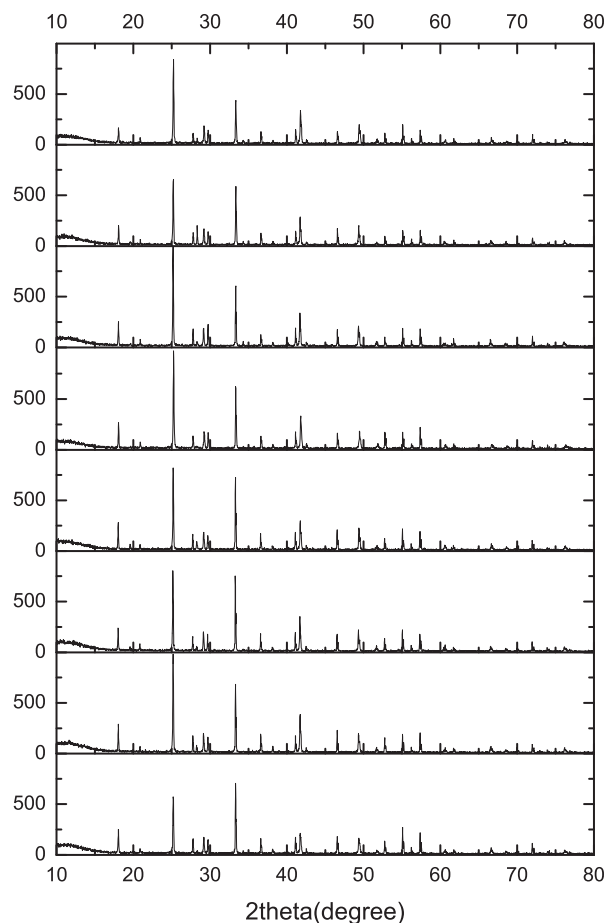


**Figure 1.** XRD patterns of YAG:Ce<sup>2+</sup> with various SrF<sub>2</sub> concentrations.

check this assumption. It produced intermediate crystal phases such as  $YAlO_3$  and  $Y_4Al_2O_9$ .

Figure 1 shows the XRD patterns of the synthesized phosphors. Crystal structures were well formed with  $SrF_2$  flux. Obviously, the synthetic route through solid-state reaction was straightforward. The selection of flux materials with proper reaction environments was the most critical factor for the maximum quantum yield. The typical emission spectrum at 450 nm and the excitation spectrum monitored at 545 nm are shown in Figure 2. The density of YAG was 4.56 g/cm<sup>3</sup>, and its effective atomic number was 35. The emission spectrum at room temperature peaked at 545 nm. The optical properties are summarized in Table 1. The quantum yield of the phosphor that was synthesized in this study was higher than those of the commercial YAG phosphors available in the market.

The main reason that the garnet phosphor recently drew attention is its stability when excited at a high photon flux. The high-power operation of the WLED requires stability (i.e. linearity at a high photon flux). In many LED phosphors, droop, a decrease in efficiency

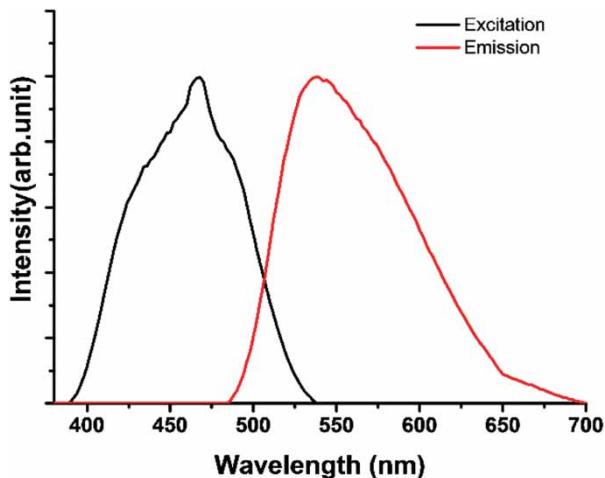


**Figure 2.** Excitation and emission at the 545 and 450 nm spectra, respectively.

**Table 1.** Optical properties of YAG:Ce phosphor.

	Commercial YAG:Ce	Present work
Dominant wavelength	550–560 nm	545 nm
Wavelength of excitation max	460 nm	460 nm
FWHM	> 100 nm	108 nm
Quantum yield	> 85%	95%
Decay time	70 ns	70 ns

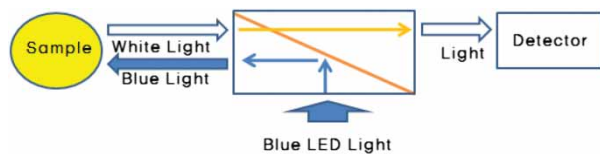


**Figure 3.** Photosaturation measurement equipment.

with increased power density, is observed. Figure 3 shows a schematic diagram of the measurement of photosaturation. The measurement was done at 298 K and 40% relative humidity. The input power of blue light onto the condensed powder was in a continuous wave from 50 to 450 mW. As shown in Figure 4, the garnet phosphors demonstrated strong linearity to the radiant flux while the  $\text{CaAlSiN}_3:\text{Eu}^{2+}$  phosphors were easily saturated. This means that the garnet phosphors are good at a high-excitation photon flux and do not show any droop during high-power operation.

The key parameters of the phosphor design for the high luminescence efficacy of the WLED are the particle size, distribution, and morphology [16,17]. It is known that the development of high-resolution displays that can achieve superior luminescence performance requires pure and ultra-fine particles. Also, the smaller particle was found to be suited for a higher color temperature, and the larger particle for a lower color temperature. Shi

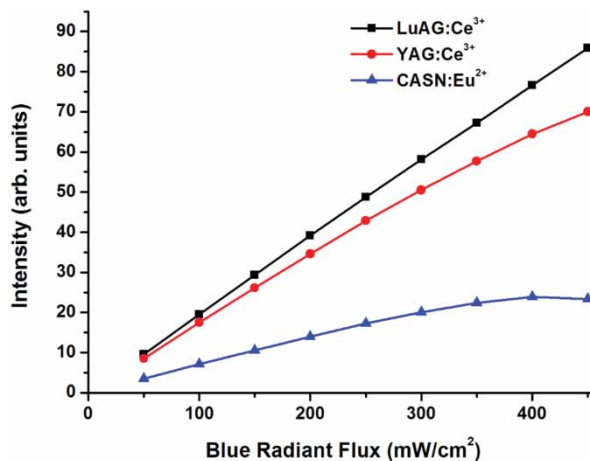


**Figure 4.** Photosaturation behavior of YAG:Ce, LuAG:Ce, and  $\text{CaAlSiN}_3:\text{Eu}^{2+}$ .

et al. showed the brightness variations when the particle size is varied in a wide range [15]. They found that the large particle (20  $\mu\text{m}$ ) and the nanoparticle (0.1  $\mu\text{m}$ ) could enhance the light extraction. This conclusion is not very convincing, however, because only one phosphor thickness and one color temperature were considered. It is very important, however, to develop a synthesis method that will allow morphology and particle size control for each device application case. In this study, the selection of flux materials with a heat treatment cycle was considered for the study purpose. A physical process such as grinding and sieve screening was added after the reaction. Through the above steps, phosphors were classified into four groups. The typical SEM image of phosphor powders and the particle size distribution for each group are shown in Figures 5 and 6, respectively. Their optical properties are summarized in Table 2.

The experiment results based on Figures 5 and 6 show that the YAG:Ce powders with 8–25  $\mu\text{m}$  diameters can be well synthesized with strontium fluoride as flux, and are well dispersed, with good photoluminescence. At the 0.7 wt%  $\text{SrF}_2$  content, the highest peak in the emission spectra appeared without any contamination. The powder size distribution could be well controlled to keep it narrow, as shown in Figure 6. In general, the small particle size of a phosphor has a larger surface area so that the luminous and quantum efficiency would be better. Table 2 shows, however, that the PL intensity increased with the particle size, and then decreased at a certain point. The easy formation of a dead layer on the phosphor surface should be considered. The results shown in Table 2 reflect the fact that the larger the particle size is, the higher the brightness, which is attributed to the integrity of the crystal lattice of the phosphor particle. In addition, the

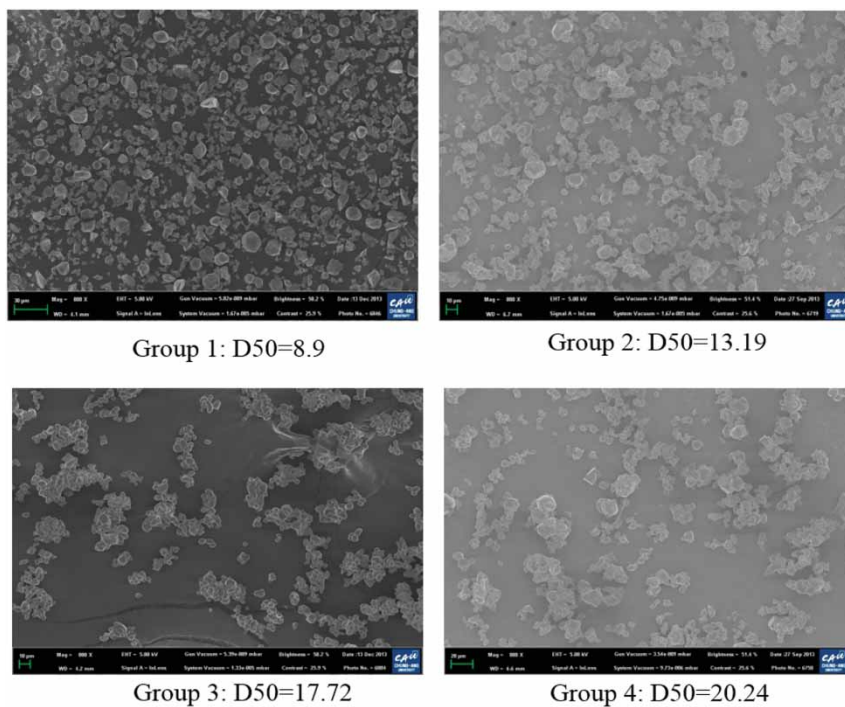


Figure 5. SEM image of YAG:Ce phosphor.

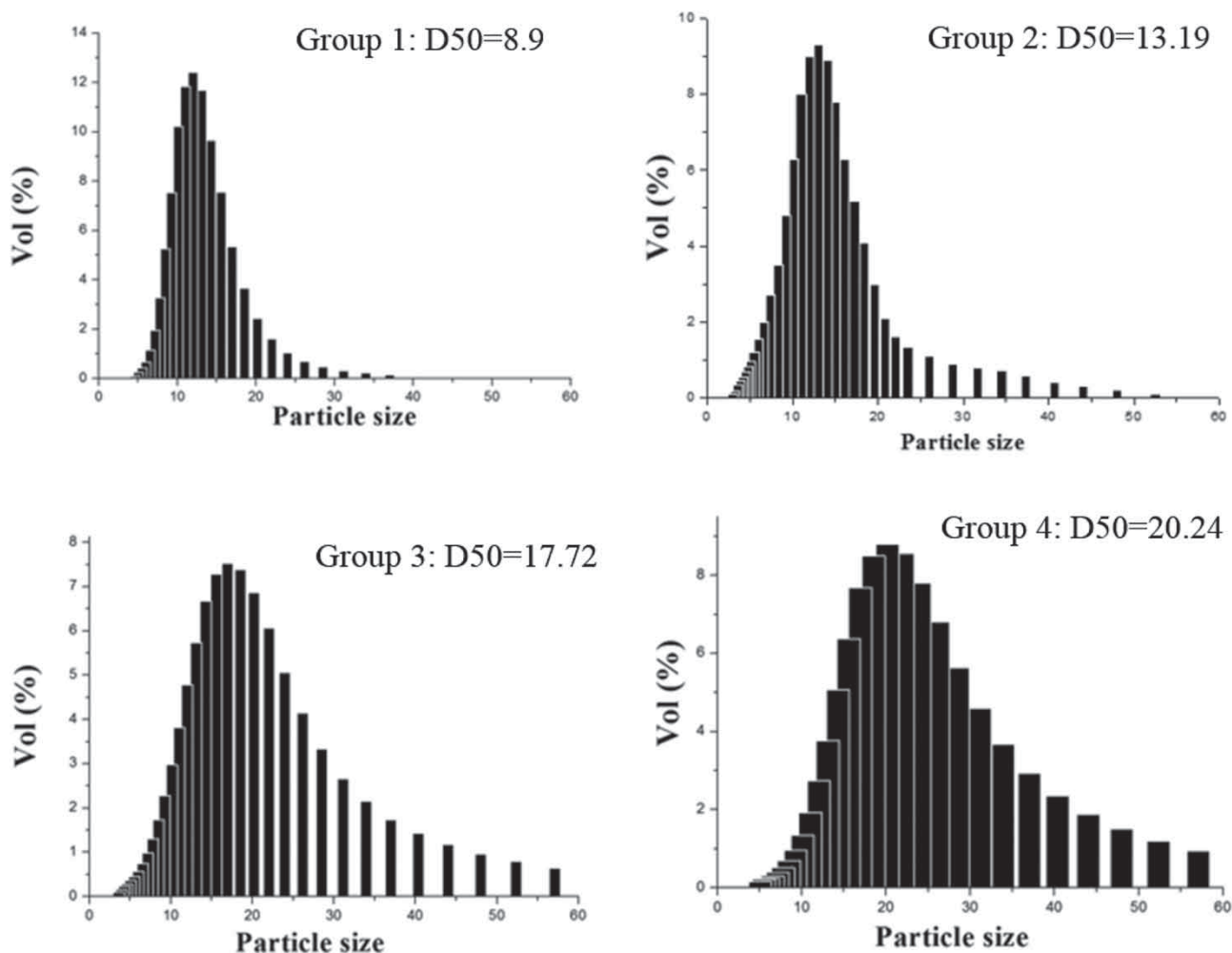


Figure 6. Particle size distribution.

**Table 2.** Optical properties of YAG:Ce LED packaging.

Phosphor	D50	Cx	Cy	Mean flux (Cy-corrected)	T/T %
Group 1	8.9	0.28	0.23178	35.48144	3.8446
Group 2	13.19	0.28	0.23672	38.70093	3.0286
Group 3	17.72	0.28	0.22256	37.48069	3.77228
Group 4	20.24	0.28	0.22164	33.94644	4.1534

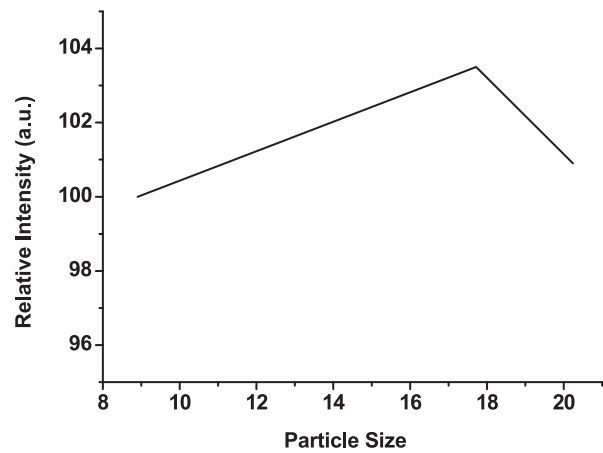
**Table 3.** Optical properties of YAG:Ce phosphor ( $\lambda_{\text{ex}} = 450 \text{ nm}$ ).

Phosphor	D50	Peak wavelength (nm)	PL intensity (%)	FWHM (nm)	CIE (x,y)
Case 1	8.9	563.6	100	117.6	(0.4578, 0.5657)
Case 2	13.19	561.6	101.7	117.8	(0.4644, 0.523)
Case 3	17.72	561.6	103.5	115.8	(0.4744, 0.5156)
Case 4	20.24	563.6	100.9	117.2	(0.4654, 0.5226)

photon flux for excitation may not effectively penetrate the particle if the particle is too big (above 25  $\mu\text{m}$ ).

To study the relationship between the phosphor powder particle size and the luminous efficacy of the WLED, blue-light-emitting chips were packaged with phosphors, which were classified into four groups according to D50. Obviously, it was expected that the size distribution and particle size would affect the packaging performance in the WLED. The direct indications of this would be the contents and the scattering. The settling rate of the larger YAG:Ce<sup>3+</sup> particles in silica can be relatively fast, and dispensing in packaging can be more difficult. It can also have a different distribution of the phosphor particles in the epoxy composite, and different contents for giving the same white point.

Table 3 shows the performance of each WLED group. As expected, the WLED had the optimum size for maximum efficacy. Very interestingly, the optimum size may be shown to be relatively smaller in packaged LED compared to the photoluminescence intensity, and the influence of the particle size is heavier in packaged LED than in powder. The backscattering and circulation of the light inside the LED package result in a high absorption loss of the emitted light. The backward propagation light may be due to the scattering of the light by the phosphor particles and the backwardly emitted portion of the phosphor-emitted yellow light. A previous work showed that about 40% of the light is transmitted through the phosphor layer while about 60% of the light is reflected backward. The backscattering and back reflection of light by the phosphor particles may be maximized with larger phosphor particle sizes. Taking into account the particle size and brightness, it was concluded that the particle size should not be too large or too small to obtain WLED with greater brightness, and that the distribution range of the particle size should be as narrow as possible. At 17  $\mu\text{m}$  D50, the luminous flux of the WLED was the maximum, as shown in Figure 7.

**Figure 7.** Luminous flux of the WLEDs with various particle sizes of D50.

#### 4. Conclusion

In this work, Ce<sup>3+</sup>-doped garnet phosphor (YAG:Ce<sup>3+</sup>) was synthesized through flux-assisted solid-state reaction to determine its advantage over other yellow-light-emitting phosphors. The synthetic procedures were found to be straightforward. Up to 95% quantum yield could be obtained, and the particle size was controlled through the heat treatment cycle and the flux material.

The synthesized garnet material was very stable. It did not have any interaction with the epoxy during the LED fabrication. First of all, the behavior of the light conversion at the high photon flux excitation was excellent. It is believed that this was due to the stable crystal structure, the low defects on the crystal surface, and the fast decay time of the Ce<sup>3+</sup> ion. Also, phosphor powders with different particle sizes were synthesized in this study and were classified into four groups with different particle size distributions (9–20  $\mu\text{m}$  on average). The luminance was relatively varied from 100% to 105.8%. Each sample was put on the blue chip, which was evaluated in advance. All the color coordinates were set to be Cx = 0.28 and Cy = 0.23 in the CIE coordinate. The amount of phosphors was expressed in T/T and was compared with the silicon quantity. As expected, the luminous flux from the WLED could reach the maximum at the average particle size of 17  $\mu\text{m}$ . It is expected that the use of the garnet phosphor will be expanded with the new application of the WLED due to the latter's availability, high quantum yield, and non-photosaturation at the high-current-injection operation.

#### Disclosure statement

No potential conflict of interest was reported by the authors.

## Funding

This work was supported by the Technological Innovation R&D Program [C0248787] funded by the Small and Medium Business Administration (SMBA, South Korea) and was partially funded by the Ministry of Trade, Industry, & Energy (MOTIE, South Korea) under the Industrial Technology Innovation Program [No. 10053623].

## Notes on contributors



**Myoung Su Jang** received his B.S. Material Science and Chemical Engineering degree from Chung-Ang University in 2015 and is now an M.S. candidate in the same institute. He has been conducting research on phosphors for WLED.



**Yong Ha Choi** received his B.S. Material Science and Chemical Engineering degree from Chung-Ang University in 2015 and is now an M.S. candidate in the same institute. He has been conducting research on phosphors for WLED.

**Shulu Wu** received her M.S. Material Science and Chemical Engineering degree from Chung-Ang University in 2014 and now works at the Chinese Academy of Science. She has been conducting research on phosphors for WLED.



**Tae Gil Lim** received his B.S. Material Science and Chemical Engineering degree from Chung-Ang University in 2016 and is now an M.S. candidate in the same institute. He has been conducting research on phosphors for WLED.



**Jae Soo Yoo** is a professor in the Department of Materials Science and Chemical Engineering at Chung-Ang University. He obtained his B.S. and M.S. degrees from Seoul National University in South Korea, and his Ph.D. degree from the University of Florida in the U.S. After graduating, he worked as a senior research engineer at Samsung Advanced Institute of Technology. Since joining Chung-Ang University in 1994, he has been working on the synthesis of luminescent materials for display applications.

## References

- [1] H. Shi, C. Zhu, J. Huang, J. Chen, D. Chen, W. Wang, F. Wang, Y. Cao and X. Yuan, *Opt. Express* **4**, 649 (2014).
- [2] L. Mancic, K. Marinkovic, B.A. Marinkovic, M. Dramicanin and O. Milosevic, *J. Eur. Ceram. Soc.* **17**, 577 (2010).
- [3] H. Jiao, Q. Ma, L. He, Z. Liu and Q.I. Wu, *Powder Technol.* **198**, 229 (2010).
- [4] N.T. Tran, J.P. You and F.G. Shi, *J. Lightwave Technol.* **27** (22), 5145 (2009).
- [5] T.L. Barry, *J. Electrochem. Soc.* **115** (11), 1181 (1968).
- [6] S.D. Jee, K.S. Choi, K.J. Choi and C.H. Kim, *Korean J. Mater. Res.* **21** (5), 250 (2011).
- [7] S.H. Kim, H.J. Lee, K.P. Kim and J.S. Yoo, *Korean J. Chem. Eng.* **23** (4), 669 (2006).
- [8] W.B. Park, Y.S. Jeong, S.P. Singh and K.S. Sohn, *ECS J. Solid State Sci. Technol.* **2** (2), R3100 (2013).
- [9] L. Chen, C.C. Lin, C.W. Yeh and R.S. Liu, *Materials* **3**, 2172 (2010).
- [10] L. Liu, R.J. Xie, N. Hirotsaki, T. Takeda, C.N. Zhang, J. Li and X. Sun, *Sci. Technol. Adv. Mater.* **8**, 329 (2016).
- [11] K. Uheda, N. Hirotsaki, Y. Yamamoto, A. Naito, T. Nakajima and H. Yamamoto, *Electrochem. Solid-State Lett.* **9** (4), H22 (2006).
- [12] J.W. Moon, B.G. Min, J.S. Kim, M.S. Jang, K.M. Ok, K.Y. Han and J.S. Yoo, *Opt. Mater. Express* **6** (3), 782 (2016).
- [13] J.W. Moon, J.S. Kim, B.G. Min, H.M. Kim and J.S. Yoo, *Opt. Mater. Express* **4** (10), 2174 (2014).
- [14] S.W. Yoon, H.K. Park, J.H. Oh and Y.R. Do, *IEEE Photonics J.* **6** (1), 1 (2014).
- [15] H.S. Jang, W.B. Im, D.C. Lee, D.Y. Jeon and S.S. Kim, *J. Lumin.* **126** (2), 371 (2007).
- [16] Y.Y. Choi, K.H. Kim, S.Y. Choi, H.D. Park and K.S. Sohn, *J. Mater. Sci. Mater. El.* **12** (3), 179 (2001).
- [17] Y. Shuai, N.T. Tran and F.G. Shi, *IEEE Photonics Technol. L.* **23** (9), 552 (2011).